Crystal Morphology and Isothermal Crystallization Kinetics of Short Carbon Fiber/Poly(ethylene 2,6-naphthalate) Composites

Li-Juan Zheng,[1] Jian-Gang Qi,[2] Qing-Hong Zhang,[1] Wen-Feng Zhou,[1] Dan Liu[1]

[1]*Computer and Information Engineering Department, Shijiazhuang Railway Institute, Shijiazhuang 050043, China*
[2]*Tian Zheng Supervising Company, Hydrogeology and Engineering Geology of Hebei Prospecting Institute, Shijiazhuang 050021, China*

Received 14 October 2007; accepted 6 November 2007
DOI 10.1002/app.27653
Published online 7 January 2008 in Wiley InterScience (www.interscience.wiley.com).

ABSTRACT: Isothermal crystallization kinetics, subsequent melting behavior, and the crystal morphology of short carbon fiber and poly(ethylene 2,6-naphthalate) composites (SCF/PEN) were investigated by using differential scanning calorimetry and polarized optical microscopy. The crystal morphology of the composites isothermally crystallized at T_c = 220°C is predominantly banded spherulites observed under polarizing micrographs, while the pattern of banded spherulites changed from ring to serration as the SCF content added into the PEN. Moreover, nonbanded spherulites formed at T_c = 210°C. The commonly used Avrami equation was used to fit the primary stage of the isothermal crystallization. The Avrami exponents n are evaluated to be 2.6–3.0 for the neat PEN and 3.7–4.0 for SCF/PEN composites, and the SCF acting as nucleation agents in composites accelerates the crystallization rate with decreasing the half-time of crystallization, and the sample with SCF component of 2% has the fastest crystallization rate. The crystallization activation energy calculated from the Arrhenius formula suggests that the adding SCF component improved the crystallization ability of the PEN matrix greatly, and the sample with of 2% SCF component has the most crystallization ability. Subsequent melting scans of the isothermally crystallized composites exhibited triple melting endotherms, in which the more the component of SCF, the lower temperature of the melting peak, indicating the less perfect crystallites formed in those composites. Furthermore, the melting peaks of the same sample are shifted to higher temperature with increasing T_c, suggesting the more perfect crystallites formed at higher T_c. © 2008 Wiley Periodicals, Inc. J Appl Polym Sci 108: 650–658, 2008

Key words: poly(ethylene 2,6-naphthalate); SCF; banded spherulites; isothermal crystallization

INTRODUCTION

Poly(ethylene 2,6-naphthalate) (PEN) is a high-performance thermoplastic polyester with a rigid naphthalene ring and a flexible aliphatic diol unit.[1–4] It has attracted considerable attention because of its superior thermal, mechanical, barrier, and chemical resistance properties compared with poly(ethylene terephthalate) (PET).[5,6] These properties make PEN useful in a wide range of applications, especially in films, magnetic tapes, and packaging materials.[7–9]

Carbon fiber in the production of polymer composites for high-technology applications is increasing rapidly because of their good mechanical, thermal, and electrical properties.[10–12] Short fibers, in particular, have the additional advantage of being able to be processed using conventional processing techniques, such as extrusion and injection molding.[13] Polymer blending is an attractive alternative for producing new polymeric materials with desirable properties without having to synthesize a totally new material The important studies on carbon fiber-reinforced polymer composites include CF/PEEK, CF/PP, CF/PEI, CF/EP, and so on.[14–19]

Studies related to the kinetics of polymer crystallization are of great importance in polymer processing, because of the fact that the resulting physical properties are strongly dependent on the morphology formed and the extent of crystallization occurring during processing. However, to our knowledge no experimental about effects of the short carbon fiber (SCF) on isothermal crystallization behavior and the crystal morphology of PEN have been reported.

In this article, isothermal crystallization kinetics, subsequent melting behavior, and crystal morphology of the SCF/PEN composites were investigated. From differential scanning calorimetry (DSC) measurements, the study on the isothermal crystallization kinetic was performed through the Avrami equation. Crystallization activation energy was calculated by Arrhenius method. Moreover, crystal morphology of the composites was studied by polarized optical microscopy (POM).

Correspondence to: L.-J. Zheng (zlj_hbr@163.com).

EXPERIMENTAL

Raw materials

The PEN homopolymer was supplied in pellet form by Honeywell (Minneapolis, MN) with an intrinsic viscosity of 0.89 dL/g measured in phenol/tetrachloroethane solution (60/40, w/w) at 30°C. SCF (M40B) used in our experiment was a PAN-based type supplied by Toray Industries (Chiba, Japan) with a diameter of 8 μm and an average length of 4 mm.

Composites preparation

PEN was dried in a vacuum oven at 120°C for 4 h and the SCF were dried in oven at 70°C for 24 h before preparing composites. PEN and SCF were mixed together with different weight ratio of SCF/PEN as following: A0: 0/100; A1: 1/99; A2: 2/98; A3: 5/95; A4: 10/90, and then melt-blended in a ZSK-25WLE (Stuttgart, Germany, WP) self-wiping, corotating twin-screw extruder, operating at a screw speed of 100 rpm and at a die temperature of 300°C. The resultant composite ribbons were cooled in cold water, cut up, re-dried before being used in measurements.

Differential scanning calorimetry characterization

The melting behaviors of five samples were studied by the Perkin–Elmer (Boston, MA) Diamond DSC instrument that calibrated with indium before performing the measurement, and the weights of all samples were ~ 8.0 mg. Samples were heated to 300°C at 100°C/min under a nitrogen atmosphere, held for 5 min to reset previous thermal history, after which all samples were immediately quenched under a cooling rate of 100°C/min to obtain the completely amorphous state of five samples, and then heating them at a rate of 10°C/min. The final heating scan was recorded.

Isothermal crystallization and subsequent melting process were performed as follows: the samples were heated at a rate of 150°C/min to 300°C, held for 5 min, and then cooled to the designated crystallization temperatures (T_c) rapidly (100°C/min). After the isothermal crystallization finished, the samples were heated to 300°C at a rate of 10°C/min. The isothermal crystallization and the final melting processes were recorded, respectively.

Polarized optical microscopy characterization

POM (59XA, Shanghai Yongheng, Shanghai, China) with a digital camera system (Panasonic wv-CP240, Tokyo, Japan) was used for observation of the crystal morphology. Samples were pressed between two glass slides with a distance of about 150 μm and first melted on a hot stage at 300°C for 10 min, and then annealing in an oven at 220 and 210°C for 4 h, and finally taking photographs under POM.

RESULTS AND DISCUSSION

Crystal morphological feature

The morphological feature of semicrystalline polymers, such as crystalline form and spherulites dimension, can be affected greatly by filling and temperature. Figure 1 shows the POM micrographs of samples at T_c = 220°C (a–d) and T_c = 210°C (e–h).

As seen in Figure 1(a), spherulites are fairly big and perfectly grown with the Maltese cross; furthermore, they have a clearly periodic ringed pattern for neat PEN. These spherulites are also known as banded spherulites. Keller and Keith have studied the origin of ringed spherulites in detail.[20,21] The formation of banded structure is attributed to lamellar twisting during growth.[22] Moreover, the spherulites dimension and banding space are constantly about 210 and 15 μm.

Figure 1(b) shows the micrographs when 1 wt % of SCF was added. It exhibits some clear Maltese cross extinction patterns and periodic banded patterns. The spherulites dimension is about 150 μm, which is smaller than that of pure PEN at T_c = 220°C. When more SCF is added in the matrix, such as shown in Figure 1(c–e), their micrographs exhibit still good Maltese cross extinction patterns and periodic serrated patterns; however, the spherulites dimension become smaller and smaller. The reason is that SCF can be acted as heterogeneous nucleus, resulting in crystals growth in a more confined space. It indicates that the more content of SCF, the smaller are the spherulites. Furthermore, the banded patterns also changes with increasing SCF: periodic ringed pattern → periodic serrated pattern → blurry serrated pattern. It is suggested that the addition of SCF influences the banded spherulites dimension and pattern strongly. As a result, the banding space of A1, A2, and A3 are almost 8 μm, which is smaller than that of neat PEN.

Blending reduced band spacing in the blends has been observed in PCL/SAN[23] and PCL/ethyl cellulose blends.[24] However, why the blending can cause narrower band spacing is still unclear. It is known that in pure crystalline polymer band spacing may depend on the following factors: chain mobility, radial growth rate of the spherulite, degree of supercooling, surface free energy, lamellar thickness, etc. The reason may be that SCF affects the lamellar twisting, chain mobility, or the surface free energy of the spherulite. Additionally, the band pattern is distorted from ring to serration, and the lamellar twisting is not as regular as those in neat PEN, indicating

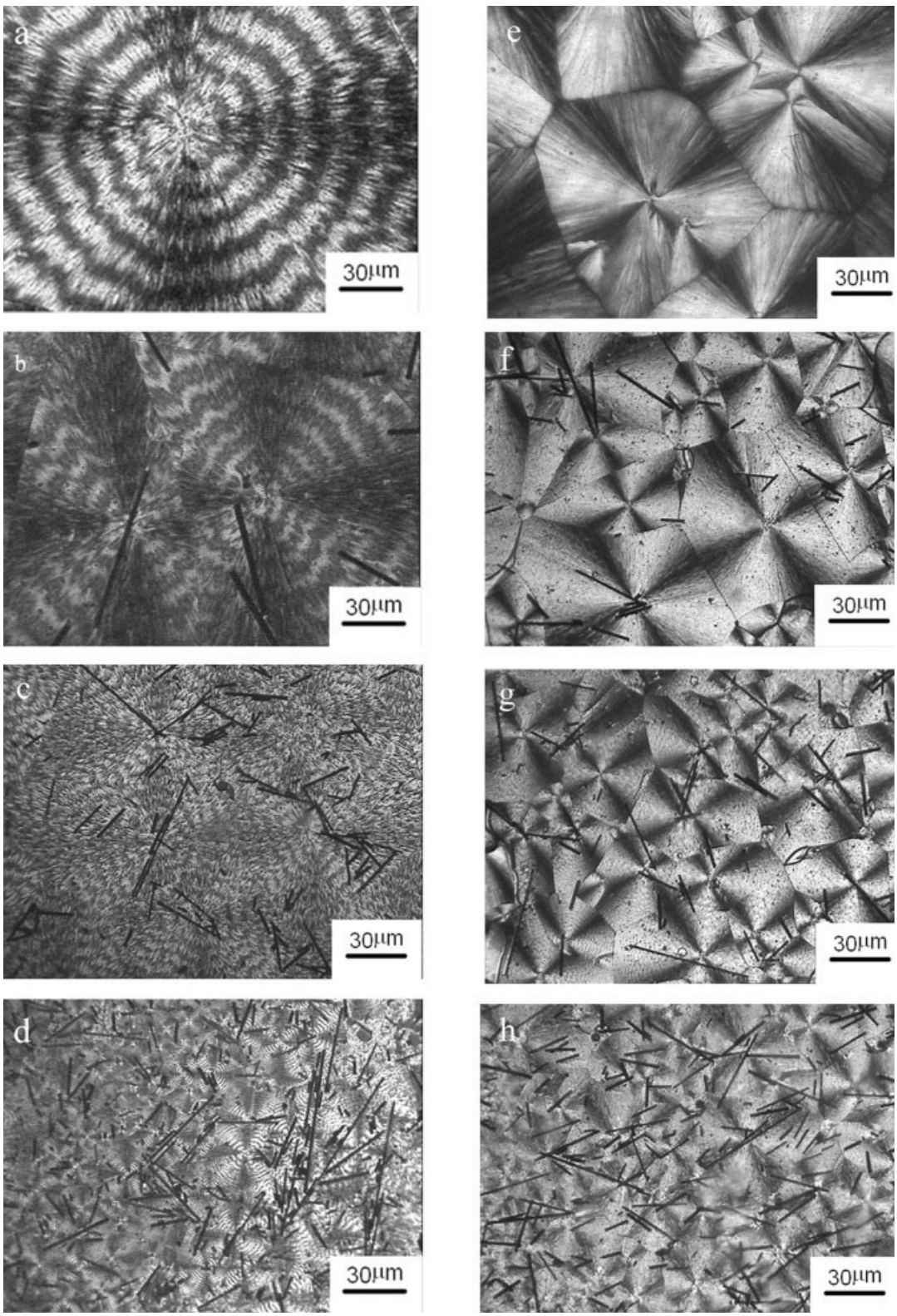

Figure 1 POM micrographs of SCF/PEN composites at 220°C: (a) A0, (b) A1, (c) A2, (d) A3 and 210°C: (e) A0, (f) A1, (g) A2, (h) A3.

that SCF has influenced the lamellar twisting because of the interfacial action and blocking effect between SCF and PEN chains.

To investigate how the temperature influences the crystal morphology, we take some micrographs of the composites isothermally crystallized at

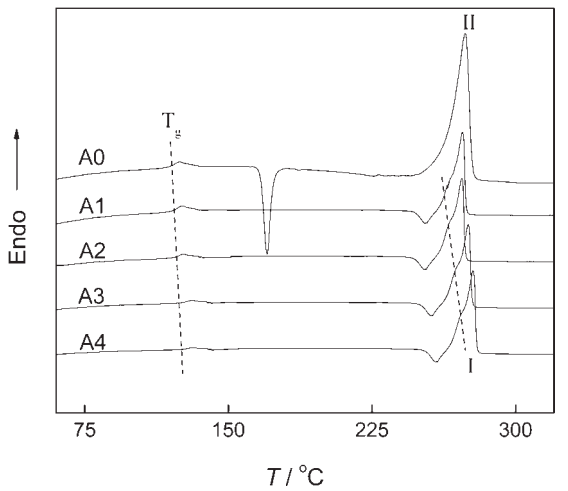

Figure 2 Melting curves at a heating rate of 10°C/min.

T_c = 210°C, and the micrographs are shown in Figure 1(e–h). The obvious changes are the disappearance of band and the decrease of the spherulites dimension compared with T_c = 220°C. The degree of supercooling ($\Delta T = T_m - T_c$) increasing with the decrease of T_c brings on the change in crystal structure or growth axis.[25,26] Moreover, the transformed temperature of the morphological change from banded to nonbanded is 213°C in this study. The spherulite diameter decreases from 210 to 120 μm for A0, 150 to 90 μm for A1, 120 to 50 μm for A2, and 70 to 25 μm for A3, respectively. The decrease in spherulite diameter is because of an increase in nucleation rate, as the crystallization temperature is reduced from 220 to 210°C.

Melting behavior

Figure 2 displays the DSC curves of glass transition, cold-crystallization, recrystallization, and melting behavior of different composites at a heating rate of 10°C/min. The parameters are listed in Table I. According to Figure 2 and Table I, the glass transition can be observed in each curve but the transitions of A1–A4 are not as sharp as that of pure PEN, even the transition of A4 becomes indistinct. T_g of SCF/PEN composites shift to higher temperature with the increasing component of SCF, e.g., T_g values shift from 125.9 to 135.1°C as SCF component increases from 0 to 10%. This can be explained by the formation of rigid amorphous phase (RAP) for the presence of SCF.[27–29] Because of besides crystalline and amorphous phases, the RAP can be formed between crystalline and amorphous layers in PEN. The RAP having distinct chain mobility from liquid-like amorphous phase could relax at a temperature higher than T_g, as only the relaxation of liquid-like amorphous chains takes place, resulting in unfreezing at a higher temperature. The interaction between SCF and PEN molecular chains results in the RAP formation, which leads to a temperature shift of the glass transition.

Furthermore, only pure PEN exhibits a sharp cold-crystallization peak (T_{cold}) at about 170.9°C, whereas no cold-crystallization peak appears in A1–A4 composite. This can be explained by the existence of the interaction between SCF and PEN molecular chains, which blocks the movement of the chain segments of PEN at this temperature. This difference is important for the product processing and product using. At the same cooling rate in processing, SCF/PEN composite can form more stable structure because of the interaction between SCF and PEN, so the product made in this process will not change its properties (e.g., dimension) when used at the temperature range of 160–180°C.

In Figure 2, the cold-crystallization peak area is smaller than the melting peak area and no recrystallization peak can be observed in the melting curve of pure PEN, which indicates at the quenching rate of 100°C/min the molten PEN molecules are frozen into amorphous state directly. Whereas the molten PEN in SCF/PEN composites are turned into a partial crystalline one at the same quenching rate because there is a recrystallization peak (T_{re}) at 252.3, 253.2, 256.1, and 258.9°C in each curve of A1–A4 composites, respectively. When the SCF/PEN composites are quenched from molten state at 100°C/min, the SCF acting as nucleus agent accelerates the nucleation rate and much microcrystallites can form immediately in composites, thus, the final sample is partially crystalline but not at absolutely amorphous state. As a result, the microcrystallites in

TABLE I
Parameters of Five Samples During the Melting Process

	First melting process						
Samples	T_g (°C)	T_{cold} (°C)	T_{re} (°C)	ΔH_c (J/g)	T_{mI} (°C)	T_{mII} (°C)	ΔH_{mI+II} (J/g)
A0	125.9	170.9	–	−30.1	–	273.3	50.9
A1	127.8	–	252.5	−20.5	268.7	273.6	42.7
A2	129.7	–	253.2	−19.1	269.1	274.4	40.8
A3	132.4	–	256.1	−18.5	269.9	274.7	38.6
A4	135.1	–	258.9	−18.0	270.0	274.8	37.6

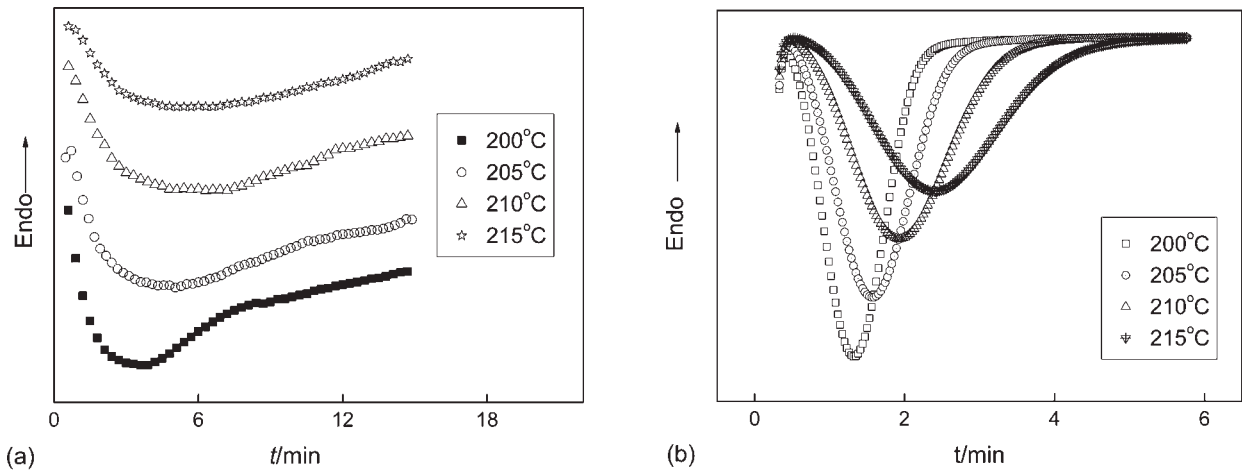

Figure 3 Heating flow versus time for isothermal crystallization at different crystallization temperatures: (a) A0, (b) A2.

composites will melt and then recrystallize to yield crystals of the better perfection or thicker lamellae during heating process.

As shown in Figure 2, the melting behaviors for the five samples are different as the composites' component varies. Obviously, the DSC curve of A0 exhibits a single melting peak (T_{mII}), whereas all A1–A4 composites show double melting peaks, T_{mI} and T_{mII}, which shift to higher temperature with an increasing amount of SCF. Peaks II and I are corresponding to the different perfect crystals or different thick lamellae formed in the recrystallization process. Moreover, the melting enthalpy (ΔH_{mI+II}) decreases gradually with the increasing component of SCF, indicating that the recrystallization degree of the composite is decreased by SCF because of its blocking effect on the arrangement of the polymer chains.

Isothermal crystallization kinetics

Isothermal crystallization behaviors

The exothermal diagrams of isothermal crystallization analysis for PEN and SCF/PEN composites are shown in Figure 3(a,b). As the crystallization temperature (T_c) increased, the exothermal peaks of each curve shifted to longer time, indicating that T_c is an important influencing factor determining the crystallization time. From the data listed in Table II, the crystallization enthalpy (ΔH_c) of neat PEN gradually decreases greatly with increasing T_c. While for A1–A4, ΔH_c increases but changes slightly with increasing T_c, indicating ΔH_c has a minor dependence on T_c. Moreover, comparing the exothermal curves of A2 with A0, they become much narrow than those of A0; in other words, the isothermal crystallization time of A2 is much shorter than that of A0 at the same T_c. These results suggest that the SCF component has been a predominant influencing factor on determining the crystallization time or the crystallization rate of the composites, and the crystallization rate is increased much by SCF.

Figure 4(a,b) shows the relative crystallinity (X_t) integrated from Figure 2 as a function of the crystallization time (t) for A0 and A2 at various isothermal crystallization temperatures (T_c). In Figure 4(a,b), the characteristic sigmoidal isothermals are shifted to right along the time axis with increasing T_c. This result indicates a progressively slower crystallization rate as T_c increase.

Another important parameter is the half-time of crystallization ($t_{1/2}$), which is defined as the time taken from the onset of the relative crystallinity until 50% completion. The dependence of $t_{1/2}$ upon T_c for

TABLE II
Kinetic Parameters of Isothermal Crystallization for Various Samples

Samples	T_c (°C)	N	$t_{1/2}$ (min)	$Z_t \times 10^{-2}$ (min^{-n})	ΔH (J/g)
A0	200	2.6	4.95	6.45	−17.7
	205	2.7	5.53	4.64	−16.2
	210	2.8	5.97	3.95	−13.6
	215	3.0	6.48	2.44	−11.3
A1	200	4.0	1.14	65.3	−44.7
	205	3.9	1.41	42.8	−46.1
	210	3.8	1.80	29.8	−46.4
	215	3.8	2.34	20.1	−46.5
A2	200	3.8	0.93	86.7	−45.5
	205	3.9	1.17	49.8	−45.8
	210	3.7	1.50	32.4	−47.0
	215	3.9	2.01	29.3	−47.6
A3	200	3.9	1.14	65.4	−46.9
	205	3.8	1.32	43.8	−47.6
	210	3.8	1.65	30.1	−47.7
	215	3.7	2.10	22.8	−49.1
A4	200	3.9	1.11	69.6	−43.4
	205	3.8	1.26	47.0	−44.3
	210	3.7	1.56	31.4	−45.6
	215	3.9	2.03	24.6	−46.1

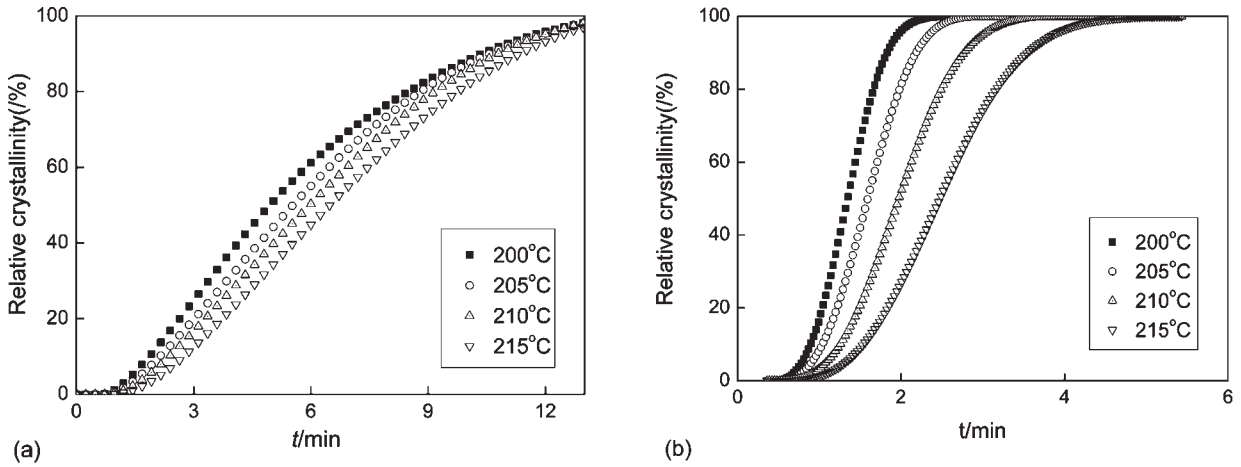

Figure 4 Relative degree of crystallinity versus time for isothermal crystallization at different crystallization temperatures: (a) A0, (b) A2.

different samples is shown in Figure 5 and the data is also listed in Table II. It is seen that $t_{1/2}$ of neat PEN increase sharply as T_c increased from 200 to 215°C. However, curves of A1–A4 show slow changes of $t_{1/2}$ with increasing T_c and the lower dependency characteristic on T_c than neat PEN. As T_c increased from 200 to 215°C, $t_{1/2}$ of neat PEN is evidently longer compared with that of A1–A4. From the above results, the SCF can act as nuclear agent to increase the crystallization rate of the composites. Furthermore, $t_{1/2}$ of A2 is smaller than that of A1, A3, and A4 at the same T_c. Although the SCF can act as nuclear agent, too much SCF colliding and intercrossing each other will slower or block the movement and arrangement of PEN chains, leading to a decrease of the crystallization rate.

Analysis based on the Avrami equation

Assuming that the relative crystallinity (X_t) increases with the crystallization time (t), the Avrami equation can be used to analyze the isothermal crystallization process of the four composites as follows[30,31]:

$$1 - X_t = \exp(-Z_t t^n) \quad (1)$$

$$\log[-\ln(1 - X_t)] = n \log t + \log Z_t \quad (2)$$

where X_t is the relative crystallinity at time t; the exponent n is a mechanism constant with a value depending on the type of nucleation and the growth dimension, and the parameter Z_t is a growth rate constant involving both nucleation and the growth rate parameters.

The plots of $\log[-\ln(1 - X_t)]$ versus $\log t$ according to eq. (2) are shown in Figure 6(a,b). The crystallization process is usually treated in two stages: the primary crystallization stage and the secondary crystallization stage. In Figure 6, it can be seen that each curve is composed of two sections. So it indicates that the neat PEN and the SCF/PEN composites exist in the secondary crystallization stage. It is generally believed that the secondary crystallization was caused by the spherulites impingement in the later stage of crystallization process.[32] The occurring time of secondary crystallization of A2 is t = 1.54 min ($\log t$ = 0.19), which is much shorter than the neat PEN (A0: t = 3.24 min, $\log t$ = 0.54) measured at the same temperature, e.g., T_c = 205°C. It is suggested that the nucleus in neat PEN grow slowly into spherulites before they impinge each other, whereas SCF can cause primary crystallization earlier because much small crystals form rapidly and then impinge each other.

The Avrami exponent n and the rate constant Z_t can readily be extracted from the Avrami plots in Figure 6. The values of n and Z_t of various samples are listed in Table II. In this work, the values of n

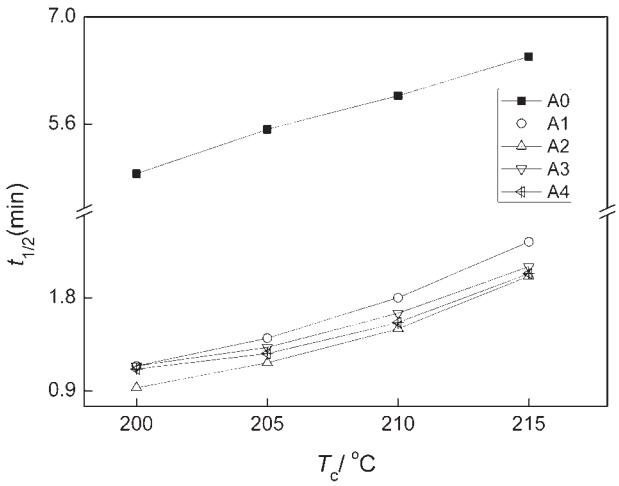

Figure 5 The $t_{1/2}$ versus T_c for various samples.

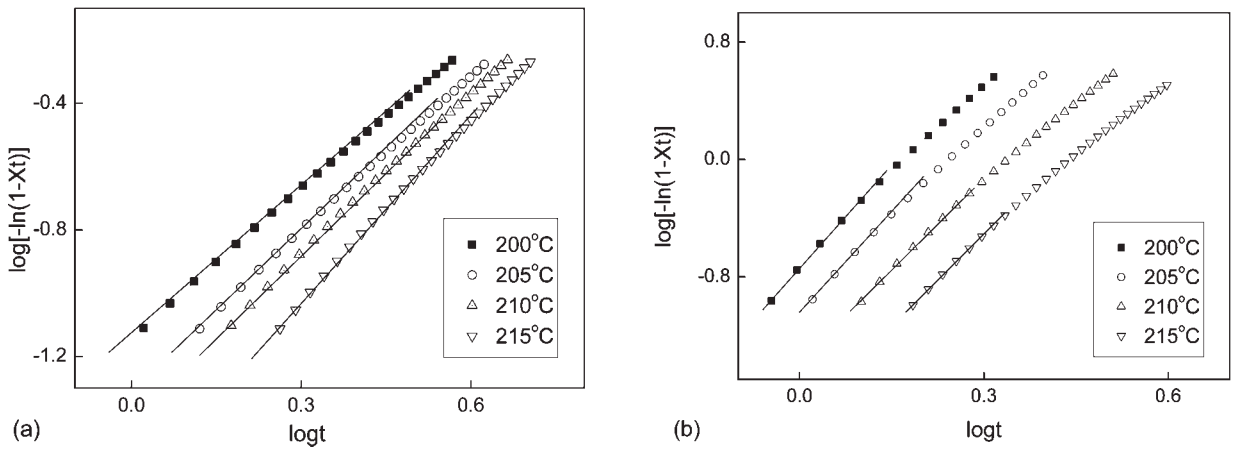

Figure 6 Plots of $\log[-\ln(1 - X_t)]$ versus $\log t$ for different composites of isothermal crystallization at indicated temperatures.

for A0 and A2 are about 2.8 ± 0.2 and 3.8 ± 0.1, which may be an average value of various nucleation types, and the growth dimensions occurred simultaneous in a crystallization process. As T_c = 215°C, the n values slightly increase with increasing the SCF component at the primary crystallization stage. For neat PEN without any heterogeneous nucleus, its nucleation type should be homogenous nucleating and its growth dimension should be a two-dimensional growth. For SCF/PEN composites with heterogeneous nucleus of SCF, the nucleation type should be mainly heterogeneous and the growth dimension should mostly be three-dimensional.

The values of Z_t for all samples decrease with increasing T_c, which indicates that Z_t is very sensitive to temperature. Z_t of A1 (42.8×10^{-2} min^{-n}), A2 (49.8×10^{-2} min^{-n}), A3 (43.8×10^{-2} min^{-n}), and A4 (47.0×10^{-2} min^{-n}) are all about 10 times of A0 (4.64×10^{-2} min^{-n}) at T_c = 205°C. This indicates that the component of SCF accelerates the crystallization rate of PEN; however, too much SCF component in the composites can induces SCF collide and intercross each other, which will slower the movement and rearrangement of PEN chain and reduce the crystallization rate.

Melting behavior of the samples annealed at different temperatures

Figure 7(a,b) present a series of DSC heating thermograms for neat PEN and SCF/PEN composites that has been annealed at different T_c. The melting parameters are summarized in Table III. As seen in Figure 7(a) and Table III, the melting endotherms of neat PEN exhibit three melting peaks. These peaks are shifted to higher temperature as T_c increases. The small melting peak I is shifted more sharply to high temperature than other two peaks. According to the similar explanations of multiple endotherms of PEN, these peaks mainly refer to the melting of

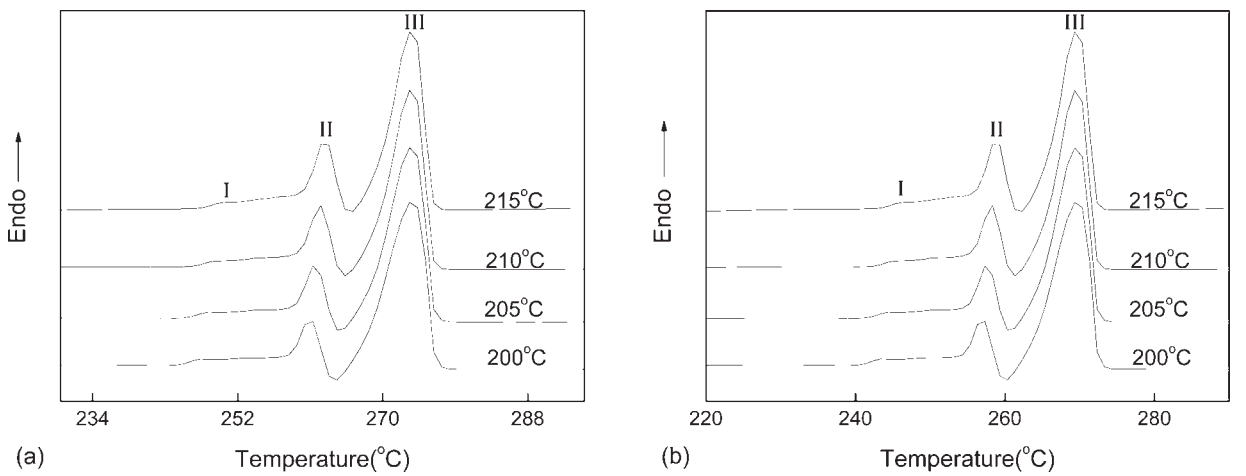

Figure 7 Melting endotherms of the four composites recorded at a heating rate of 10°C/min after isothermal crystallization at the specified temperatures.

TABLE III
Melting Endotherms Parameters of Various Samples

Samples	T_c (°C)	T_m (°C) I	II	III	ΔH_f (J/g)
A0	200	244.1	258.9	273.1	35.7
	205	245.8	259.5	273.4	36.8
	210	247.7	260.4	273.4	39.6
	215	248.5	260.8	273.4	40.1
A1	200	243.0	257.4	272.8	47.0
	205	244.2	257.9	272.0	48.4
	210	245.1	258.4	273.1	48.6
	215	246.5	259.3	273.1	49.5
A2	200	243.2	257.0	272.5	50.3
	205	244.3	257.5	272.6	50.4
	210	245.2	258.3	272.6	50.8
	215	246.3	258.7	272.6	51.9
A3	200	242.8	256.5	272.0	49.9
	205	243.2	257.4	272.0	50.4
	210	244.8	257.6	272.1	50.5
	215	245.3	258.3	272.3	49.6
A4	200	242.4	256.2	272.9	45.9
	205	242.9	256.7	272.0	47.9
	210	244.2	257.4	272.0	47.9
	215	244.5	258.3	272.1	46.5

the crystals with different perfection.[33] The occurrence of peak I at lower temperature is attributed to the microcrystallite formation. Peak II corresponds to the primary crystal with perfect form. While peak III is attributed to the melting of the most perfect crystals. So the result, that the peaks are shifted to higher temperature with T_c increases indicates that more perfect crystals have formed at higher T_c.

As seen in Figure 7(b) and Table III, the melting endotherms of SCF/PEN composites also exhibit three melting peaks. These peaks are also shifted to higher temperature as T_c increases. Comparing the peaks for A0–A4 at the same T_c, e.g., T_c = 215°C, it can be concluded that the more SCF component in composites, the lower is the peak value. It might be concluded that the SCF can improve the formation of the microcrystallite with poor morphology; furthermore, more imperfect crystals might be formed with increasing the SCF component. The total melting enthalpy (ΔH_f) is calculated from the beginning of the melting of peak II to the end of the melting of peak III. ΔH_f of the SCF/PEN is higher than that of neat PEN at the same T_c, which indicates that the SCF component can improve the crystallization of the PEN matrix during the isothermal crystallization process and the crystallinity is increased accordingly.

Crystallization activation energy

The crystallization process of the neat PEN and SCF/PEN composites is assumed to be thermally activated. The crystallization rate parameters K_t can be approximately described by the following Arrhenius equation[34]:

$$K_t^{1/n} = K_0 \exp(-\Delta E/RT_c) \quad (3)$$

$$(1/n)\ln K_t = \ln K_0 - \Delta E/RT_c \quad (4)$$

where K_0 is the temperature independent preexponential factor, R is the gas constant, and ΔE is the crystallization activation energy. ΔE can be determined by the slope coefficient of plots with $(1/n)\ln K_t$ versus $1/T_c$ in eq. 4, which is shown in Figure 8.

In this case, the ΔE values of A0–A4 are −21.1, −39.8, −56.0, −46.7, and −44.4 kJ/mol, respectively. Because it has to release energy when the molten fluid transformed to the crystalline state, the value of ΔE is negative on the basis of the concept of the heat quantity in physical chemistry. The value of ΔE has the minimum value as the SCF in PEN matrix is 2 wt %. This result suggests that the addition of SCF into PEN matrix can induce the heterogeneous nucleation and mostly increase the crystallization ability of PEN during the crystallization processes; however, too much SCF colliding and intercrossing each other will slower the movement and rearrangement of PEN chain, so the value of ΔE decreases when the content of SCF exceeds 2 wt %.

CONCLUSION

PEN/SCF composites prepared by melt-extruding are investigated on its isothermal crystallization kinetics, subsequent melting behavior, and crystal morphology by using DSC and POM. The crystal morphology of the composites is predominantly banded spherulites observed under polarizing micrographs; furthermore, the pattern of banded spherulites changed from ring to serration at T_c = 220°C.

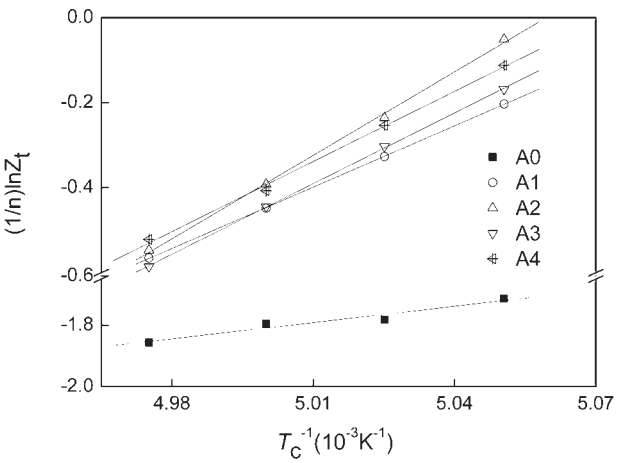

Figure 8 Plots of $(1/n)\ln Z_t$ versus $1/T_c$.

However, nonbanded spherulites appeared at T_c = 210°C. The degree of supercooling increases with the decreasing of T_c brings on the change in crystal structure or growth axis. The Avrami equation was used to fit the primary stage of the isothermal crystallization. The Avrami exponents n were evaluated to be 2.6–3.0 for the neat PEN and 3.7–4.0 for SCF/PEN composites. The results show that SCF acting as nucleation agents in composites accelerated the crystallization rate with decreasing the half-time of crystallization. Moreover, the sample in which SCF component is 2% has the least $t_{1/2}$. Subsequent melting scans of the isothermally crystallized composites all exhibited triple melting endotherms, in which more the component of SCF, the lower temperature of the melting peak. Furthermore, the melting peaks of the same sample are shifted to higher temperature with increasing T_c. The crystallization activation energy calculated from the Arrhenius' formula and the sample in which SCF component is 2% has the least value. Therefore, the addition of SCF component improved the crystallization ability of the PEN matrix greatly.

References

1. Lee, W. D.; Yoo, E.; Im, S. S. Polymer 2003, 44, 6617.
2. Run, M. T.; Wang, Y. J.; Yao, C. G.; Zhao, H. C. J Appl Polym Sci 2007, 103, 3316.
3. Schoukens, G.; Verschuere, M. Polymer 1999, 40, 3753.
4. Patcheak, T. D.; Jabarin, S. A. Polymer 2001, 42, 8975.
5. Run, M. T.; Wang, Y. J.; Yao, C. G.; Gao, J. G. Therm Acta 2006, 447, 13.
6. Schoukens, G.; Clerck, K. D. Polymer 2005, 46, 845.
7. Karayannidis, G. P.; Papachristos, N.; Bikiaris D. N.; Papageorgiou, G. Z. Polymer 2003, 44, 7801.
8. Pongpipat, K.; Pitt, S. Eur Polym J 2005, 41, 1561.
9. Douillard, A.; Hakme, C.; David, L.; Stevenson, I.; Boiteux, G.; Seytre, G.; Kazmierczak, T.; Galeski, A. J Appl Polym Sci 2007, 103, 395.
10. Daniel, A. B.; Jimmy, C. M. P.; Jean, B. D. Carbon 1999, 37, 1929.
11. Tsotra, P.; Friedrich, K. Compos Sci Technol 2004, 64, 2385.
12. Das, N. C.; Chaki, T. K.; Khastgir, D. Carbon 2002, 40, 807.
13. Ying, X.; Hisako, I.; Yue, Z. B.; Matsuo, M. Carbon 2004, 42, 1699.
14. Chi, W.; Liu, C. R. Polymer 1999, 40, 289.
15. Sari, N.; Sinmazcelik, T. Mater Des 2007, 28, 351.
16. Kaynak, C.; Orgun, O.; Tincer, T. Polym Test 2005, 24, 455.
17. Lee, J.; Soutis, C. Compos Sci Technol 2007, 67, 2015.
18. Erwin, M. W.; Freddy, Y. C.; Xiao, H.; Wong, S. C. Polymer 2007, 48, 3183.
19. Nam, G. Y.; Yong, G. W.; Sung, C. K. Polymer 2004, 45, 6953.
20. Keller, A. J Polym Sci 1959, 39, 151.
21. Keith, H. D.; Padden, F. J. J Polym Sci Part B: Polym Phys 1987, 25, 2265.
22. Keith, H. D. Macromolecules 1982, 15, 114.
23. Wang, Z. G.; Wang, X. H.; Yu, D. H.; Jiang, B. Z. Polymer 1997, 38, 5897.
24. Huang, Y. P.; Luo, X. L.; Ma, D. Z. Eur Polym J 2001, 37, 2153.
25. Sabino, M. A.; Feijoo, J. L.; Mulle, A. J. Macromol Chem Phys 2000, 201, 2687.
26. Sabino, M. A.; Feijoo, J. L.; Mulle, A. J. Polym Degrad Stab 2001, 73, 541.
27. Hong, P. D.; Chung, W. T.; Yeh, W. J.; Lin, T. L. Polymer 2002, 43, 6879.
28. Sumod, K.; Kalika, D. S. Poymer 2006, 47, 7085.
29. Wu, T.; Li, Y.; Wu, Q.; Song, L.; Wu, G. Eur Polym J 2005, 41, 2216.
30. Huang, H.; Gu, L. X.; Ozaki, Y. Polymer 2006, 64, 104.
31. Jeziorny, A. Polymer 1978, 19, 1142.
32. Liu, T.; Mo, Z.; Wang, S. Polym Eng Sci 1997, 37, 568.
33. Gao, X.; Hou, W. M.; Zhou, J. J.; Li, L.; Zhao, L. Q. Macromol Mater Eng 2004, 289, 174.
34. Cebe, O.; Hong, S. D. Polymer 1986, 27, 1183.